PNAS
www.pnas.org

Supplementary Information for

c-di-AMP, a likely master regulator of bacterial K^+ homeostasis machinery, activates a K^+ exporter

Tatiana B. Cereija[a,b], João P. L. Guerra[a,b,1], João M. P. Jorge[a,b], João H. Morais-Cabral[a,b,2]

Proc Natl Acad Sci U S A. 2021 Apr 6;118(14):e2020653118. doi: 10.1073/pnas.2020653118.

[a] IBMC – Instituto de Biologia Molecular e Celular, Universidade do Porto, Portugal
[b] i3S – Instituto de Investigação e Inovação em Saúde, Universidade do Porto, Portugal

[1] Current address: UCIBIO-Requimte, Departamento de Química, Faculdade de Ciências e Tecnologia, Universidade Nova de Lisboa, Portugal
[2] Corresponding author

Correspondence should be addressed to: João H. Morais-Cabral (i3S, Rua Alfredo Allen, 208, 4200-135 Porto, Portugal; Tel. +351 226 074 900; E-mail: jcabral@ibmc.up.pt)

This PDF file includes:

Extended Materials and Methods
Figures S1 to S12
Tables S1 to S3
SI References

Extended Materials and Methods

Cloning and site-directed mutagenesis

Genes coding for KhtTU or KhtT were amplified by PCR from *Bacillus subtilis* strain JH642 genomic DNA using the primer pair *khtTU_pQE60_fw*/*rv* (for *khtTU*) and *khtT_pRSFDuet_fw*/*rv* (for *khtT*) and cloned into the NcoI/BgI II restriction sites of the pQE60 (producing pQE60-*khtTU* expression vector) or BamHI/NotI restriction sites of pRSFDuet (producing pRSFDuet-*khtT*). The N-domain (ending at G68) and C-domain of KhtT (starting at A78) were cloned into pET24d using the primer pairs *N-KhtT_fw/rv* (producing pET24d-N_{His}-*khtT*) and *C-KhtT_fw/rv* (producing pET24d-C_{His}-*khtT*), respectively. Genes coding for KhtU or KhtTU were also amplified using the primer pairs *khtU_pBS0E_fw*/*rv* (for *khtU*) or *khtT_pBS0E_fw*/*khtU_pBS0E_rv* (for *khtTU*), and cloned into XbaI/PstI restriction sites of pBS0E (Bacillus Genetic Stock Center, BGSC) (1), producing the vectors pBS0E-*khtU* and pBS0E-*khtTU*, respectively. The vectors pQE60-$khtT_{His}U$, pQE60-$khtT_{R110A}U$, pBS0E-$khtT_{R110A}U$, pRSFDuet-$khtT_{R110A}$ and pRSFDuet-*N-khtT* were generated by site-directed mutagenesis using pQE60-*khtTU*, pBS0E-*khtTU* or pRSFDuet-*khtT* as templates and the primer pairs $khtT_{His}U$*_fw*/*rv* (for pQE60-$khtT_{His}$/*U*), *khtT_R110A_fw*/*rv* (for pQE60-$khtT_{R110A}U$, pBS0E-$khtT_{R110A}U$ and pRSFDuet-$khtT_{R110A}$), and *N-KhtT-stop_fw*/*rv* (for pRSFDuet-*N-khtT*). See primer sequences in Table S2.

Expression and purification of KhtT variants

Escherichia coli BL21 (DE3) cells transformed with pRSFDuet-*khtT* (for full-length KhtT), pRSFDuet-$khtT_{R110A}$ (for the $KhtT_{R110A}$ mutant), pRSFDuet-*N-khtT* (for N-domain of KhtT with cleavable tag, N-KhtT), pET24d-N_{His}-*khtT* (for the C-terminal hexahistidine tagged N-domain of KhtT, N_{His}-KhtT), pET24d-C_{His}-*khtT* (for the C-terminal hexahistidine tagged C-domain of KhtT, C_{His}-KhtT) or pQE60-$khtT_{His}U$ (for the C-terminal hexahistidine tagged KhtT, $KhtT_{His}$) were grown in LB supplemented with 50 μg mL^{-1} kanamycin (for cells transformed with pRSFDuet- or pET24d-based constructs) or 100 μg mL^{-1} ampicillin (for pQE60-based vector) at 37°C to an OD_{600nm} of ~0.8. Protein expression was induced with 0.5 mM isopropyl *β*-D-1-thiogalactopyranoside (IPTG). After 3h growth, cells were harvested, resuspended in 50 mM Tris-HCl pH 8.0, 150 mM KCl, 1 mM phenylmethylsulfonyl fluoride (PMSF), 1μg mL^{-1} leupeptin and 1μg mL^{-1} pepstatin A and lysed using an Emulsifex-C5 cell cracker (Avestin). Lysate was clarified by centrifugation and added to an immobilized metal-affinity column, pre-equilibrated with 50 mM Tris-HCl pH8.0, 150 mM KCl, 10 mM Imidazole. Proteins were eluted with 50 mM Imidazole in 50 mM Tris-HCl pH 8.0, 150 mM KCl, except for $KhtT_{His}$ for which 150 mM Imidazole was used. The hexahistidine tag of KhtT, $KhtT_{R110A}$ and N-KhtT was removed by digestion with bovine *α*-thrombin (1:1000 weight ratio) at 4°C during overnight dialysis against 20 mM Tris-HCl pH 8.0, 150 mM KCl (dialysis buffer). $KhtT_{His}$, N_{His}-KhtT and C_{His}-KhtT were also dialyzed but without addition of *α*-thrombin. Untagged KhtT, $KhtT_{R110A}$ or N-KhtT were separated from any tagged molecules by a second immobilized metal-affinity chromatography step using the same experimental conditions described above. Proteins were concentrated and loaded into a Superdex 200 10/300 GL (for KhtT, $KhtT_{R110A}$ and $KhtT_{His}$) or Superdex75 10/300 GL (for N-KhtT and C_{His}-KhtT) column (GE Healthcare) equilibrated with 20mM Tris-HCl pH 8.0, 150 mM KCl. Fractions containing pure protein were pooled and concentrated. N_{His}-KhtT was concentrated after dialysis without an additional purification step. Protein concentration was estimated by measuring its absorbance at 280 nm and using the extinction coefficients calculated with ExPASY tool Protparam. Purified proteins were flash-frozen in liquid nitrogen and kept at -80ºC until needed.

Expression and purification of selenomethionine-containing KhtT

E. coli B834 (DE3) cells transformed with pRSFDuet-*khtT* were grown in 50 ml LB medium overnight at 37ºC. Cells were collected, washed three times with sterile deionized water and used to

inoculate 1 L of SelenoMethionine Medium (Molecular Dimensions). Cell growth, protein expression and purification were performed as prescribed above for full-length KhtT, except for the addition of 1 mM TCEP to all buffers used.

Isothermal titration calorimetry

Recombinant KhtT or $KhtT_{R110A}$ were dialyzed overnight against 50 mM HEPES pH 8.0 (for KhtT) or pH 7.5 (for KhtT and $KhtT_{R110A}$), 150 mM KCl. Dialyzed proteins were centrifuged (30 min at 12,000 *g* and 4ºC) to remove any aggregates and c-di-AMP or c-di-GMP solutions were prepared by diluting stock aliquots into the respective dialysis buffer. Protein concentration was re-determined as before. Nucleotide concentrations were determined by measuring absorbance at 259 nm using the extinction coefficient 27.0 L $mmol^{-1}$ cm^{-1} (for c-di-AMP) or at 253 nm using the extinction coefficient 23.7 L $mmol^{-1}$ cm^{-1} (for c-di-GMP). Titrations were performed in a MicroCal VP-ITC instrument (GE Healthcare) at 25ºC (except for a titration of KhtT with c-di-GMP and of $KhtT_{R110A}$ with c-di-AMP also performed at 15ºC). At pH 8.0, the following experiments were performed: 1) 18, 30 or 30 μM KhtT in the cell titrated with 152, 300 or 311 μM ligand samples in the syringe, respectively; 2) 6 μM c-di-AMP (cell) titrated with 175 μM KhtT (syringe); 3) 35 μM KhtT (cell) titrated with 308 μM c-di-GMP (syringe); 4) 34 μM KhtT (cell) titrated with 291 μM c-di-GMP (syringe) at 15ºC. At pH 7.5, the following experiments were performed: 1) 18.4, 17.8 or 15.8 μM KhtT (cell) titrated with 198, 136 or 131 μM c-di-AMP (syringe); 2) 17.5 μM $KhtT_{R110A}$ (cell) with 133 μM c-di-AMP (syringe); 3) 19.2 μM KhtT (cell) with 134 μM c-di-GMP (syringe) at 15ºC. Data were visualized and analyzed with *Origin 7 Software* (by OriginLab) using a single-site binding model.

Thermal shift assay

Melting temperatures of KhtT and $KhtT_{R110A}$ were determined using a thermal shift (Thermofluor) assay. Protein samples (12 μM final concentration) were mixed with 5x SYPRO Orange (Life Technologies) in 20 mM Tris-HCl pH 8.0, 150 mM KCl in the presence or absence of 1 mM c-di-AMP or c-di-GMP (to evaluate the impact of the nucleotides) or in 20 mM Bis-Tris propane pH 8.5 or 9.0, 150 mM KCl (to evaluate the impact of pH) and loaded into white 96-well PCR plates (Bio-Rad) sealed with Optical Quality Sealing Tape (Bio-Rad). The plate was heated from 25 to 95ºC in 0.5ºC steps with 30 s hold time per step on a iCycler iQ5 Multicolor Real-Time PCR Detection System (Bio-Rad) and fluorescence was followed using Cy3 dye filter (545 nm excitation/585nm emission). Each experiment was performed in triplicate, except for those without nucleotide which were performed in quadruplicate. Melting curves were analyzed using the CFX Manager software (Bio-Rad) and the melting temperature was determined as the inflection point of the melting curve.

Crystallization of KhtT variants

Initial crystallization conditions for N-terminal domain (N-KhtT) and full-length KhtT were determined at 4 and 20°C using commercial sparse-matrix crystallization screens. Sitting-drop vapor-diffusion experiments were set up in 96-well CrystalQuick plates using an Oryx 4 crystallization robot (Douglas Instruments). Drops consisted of equal volumes (0.3 μL) of KhtT (at 8-10 mg mL^{-1} in 20 mM Tris-HCl pH 8.0, 150 mM KCl supplemented with 1 mM c-di-AMP) or N-KhtT (at 13.3 mg mL^{-1} in 20 mM Tris-HCl pH 8.0, 150 mM KCl) protein and crystallization solutions, equilibrated against 40 μL reservoir solution. The high resolution KhtT:c-di-AMP crystals were obtained in condition E6 of JBScreen Basic 3 crystallization screen (Jena Bioscience) at 4ºC. They were reproduced using MRC Maxi 48 well plates with drops composed of equal volumes (1 μL) of protein (at 10 mg mL^{-1} in 20 mM Tris-HCl pH 8.0, 150 mM KCl, 1 mM c-di-AMP) and crystallization solutions equilibrated against 150 μL 100 mM sodium acetate pH 4.6, 260 mM calcium chloride, 15% (*v*/*v*) 2-propanol. SeMet-KhtT crystals were obtained in similar conditions but from a 10 mg mL^{-1} protein solution in 20 mM Tri-HCl pH 8.0, 150mM KCl, 1 mM TCEP, 1 mM c-di-AMP using 100 mM sodium acetate pH 4.6, 200 mM calcium chloride, 17.5% (*v*/*v*) 2-propanol as precipitant

solution. Crystals for the low-resolution KhtT structure were obtained in ammonium-containing solutions at 4ºC and reproduced as previously described using 100 mM Tris-HCl pH 8.5, 2.2 M ammonium sulfate as precipitant solution. Crystals obtained in the 2-propanol-containing crystallization solutions were cryo-protected with perfluoropolyether cryo oil (Hampton Research), while those obtained from ammonium-containing solutions were cryo-protected with 30% (*w*/*v*) glucose in reservoir solution supplemented with ~1 mM c-di-AMP prior to flash-cooling in liquid nitrogen.
Crystals of N-domain alone (N-KhtT) were obtained in condition B12 JBScreen Basic (Jena Bioscience) and reproduced from drops composed of equal volumes (1 µL) of protein (at 13.3 mg mL^{-1} in 20 mM Tris-HCl pH 8.0, 150 mM KCl) and crystallization solution equilibrated against 150 µL 100 mM Bis-Tris propane pH 6.5, 200 mM ammonium sulfate, 35% PEG MME 2000. These crystals were frozen directly in liquid nitrogen. N-KhtT crystals were also obtained in condition H9 of PACT premier crystallization screen (Molecular Dimensions; 200 mM KNa tartrate•$4H_2O$, 100 mM Bis-tris propane pH 8.5, 20% PEG 3350) and cryo-protected with perfluoropolyether cryo oil (Hampton Research) prior to flash-freezing in liquid nitrogen. Finally, N-KhtT crystals were also obtained in solutions G10 and G11 JBScreen Basic crystallization screen (Jena Bioscience) and reproduced as described above using 100 mM HEPES pH 7.5, 1.6 M ammonium sulfate as precipitant solutions. These crystals were cryoprotected with precipitant solution supplemented with 15% (*v*/*v*) glycerol before being flash-frozen in liquid nitrogen. All crystals of the N-KhtT were obtained at 20ºC.

Data collection and processing
Diffraction data were collected from cryo-cooled (100 K) single crystals at beamlines XALOC of ALBA (Barcelona, Spain) and PROXIMA-1 of the French National Synchrotron Source (SOLEIL, Gif-sur-Yvette, France). Data sets were processed with *XDS* (2) and reduced with utilities from the *CCP4* program suite (3). X-ray diffraction data collection and processing statistics are summarized in Table S1.

Structure determination, model building and refinement
The high-resolution structure of KhtT in complex with c-di-AMP was solved by single-wavelength anomalous diffraction (SAD), using the anomalous signal of selenium at the *K*-absorption edge and the *SHELXC*/*SHELXD*/*SHELXE* pipeline (4) and NCS-averaging. The N-domain of KhtT was built from the SAD maps but the C-domain was restricted to a fraction consisting of the first two β-strands. Improvement of the electron-density maps, in particular in the C-domain region, was achieved by 8-fold NCS averaging performed with *DMmulti* (*CCP4* package) using separate NCS masks for the N-domain of KhtT and for a trimmed C-domain of KtrA (PDB code: 4XTT), which has a similar structure to the C-terminal domain of KhtT (5), calculated in *MAMA* (6). The solvent mask used was calculated in *NCSmask* (*CCP4* package). Alternating cycles of model building with *Coot* (7) and refinement with *PHENIX* (8) were performed until model completion. The low-resolution structure of KhtT and the N-KhtT structures were solved by molecular replacement in *Phaser* (9) using as models, residues 1 to 67 and 77 to 159 for the low-resolution KhtT and residues 1 to 67 for N-KhtT. Refined coordinates and structure factors were deposited at the Protein Data Bank (10). High-resolution and low-resolution KhtT: 7AGV and 7AHM, respectively; N-KhtT at pH 6.5, pH 7.5 and pH 8.5: 7AGW, 7AHT and 7AGY, respectively. Refinement statistics are summarized in Table S1.

Analysis of crystallographic structures
Molecular models were superposed with *SUPERPOSE* (11) and secondary structure elements were identified with *PROMOTIF* (12). Intra-dimer interface area was determined using *PISA* (13). Figures depicting crystallographic models were created with *PyMOL* (Schrödinger).

Analysis of amino acid sequence of KhtT

Evolutionary conservation scores were calculated with *ConSurf* (14). Alignment of amino acid sequences were performed with *Clustal Omega* (15, 16).

Preparation of everted membrane vesicles

KNabc cells transformed with pQE60-*khtTU* (for KhtTU- or KhtU-vesicles), pQE60-*khtT$_{His}$U*, pQE60-*KhtT$_{R110A}$U* or pQE60 (for empty vesicles) were grown at 37°C in LB to OD_{600nm} of ~0.9. Protein expression was induced with 0.5 mM IPTG for 3h. Cells were harvested and everted membrane vesicles prepared as previously described (17) in 20 mM HEPES pH 7.0 (for preparation of KhtTU-, KhtT$_{R110A}$U-, KhtT$_{His}$U- or empty vesicles) or 20 mM Tris-HCl pH 8.0 (for preparation of KhtU-vesicles from pQE60-*khtTU* or pQE60-*khtT$_{R110A}$U*), 140 mM choline chloride, 0.5 mM DTT, 250 mM sucrose (vesicle buffer). Briefly, cells were washed once in vesicle buffer and lysed by a single passage through a French press cell at 4,000 psi. After removal of unbroken cells by a 5,000 *g* centrifugation at 4ºC for 15 min, everted vesicles were collected by ultracentrifugation at 100,000 *g* and 4ºC for 1h. Everted vesicles were washed twice with vesicle buffer by gently resuspending the pellet in vesicle buffer and pelleting by ultracentrifugation at 100,000 *g* and 4ºC. Washed vesicles were resuspended in 1 mL of vesicle buffer per gram of original wet cell weight, flash-frozen in liquid nitrogen and kept at -80ºC until needed.

Antiport Assays

Fluorescence-based flux assay was performed at room temperature in a FluoroMax-4 spectrofluorometer (Horiba) with excitation at 410 nm and emission at 480 nm and 2 nm slits for both. Assays were performed in 15 mM Tris-HCl pH 7.5, pH 8.0 or pH 8.5, 140 mM choline chloride, 5 mM $MgCl_2$. Total protein concentration in everted vesicles was determined using Pierce BCA Protein Assay Kit (ThermoFisher Scientific) and BSA as standard. All flux assays were performed by diluting 200 µg of total protein everted vesicles in 1.5 mL of assay buffer containing 2 µM 9-amino-6-chloro-2-methoxyacridine (ACMA). Assays were started by adding 4 mM sodium lactate (dissolved in the assay buffer) to promote a respiration-generated ΔpH. Proton efflux was then induced by adding 50 mM KCl (unless otherwise noted). Nucleotides were added to vesicles immediately before sodium lactate. For c-di-AMP titrations, nucleotide was added to a final concentration that varied between 206 nM to 40 µM for assays at pH 7.5, from 12 nM to 40 µM for assays at pH 8.0 and from 12 nM to 17.8 µM for assays at pH 8.5. Although higher concentrations would be necessary to obtain a complete the titration curve at pH 7.5, very high concentration of c-di-AMP affected the assay and were not used. The sensitivity of KhtT$_{His}$U- or KhtT$_{R110A}$U-vesicles to c-di-AMP was evaluated with and without 15 µM c-di-AMP at pH 8.5. Control experiments were also performed with empty vesicles at pH 7.5 and 8.5 in absence and in presence of 25 µM c-di-AMP. Recombinant KhtT (0.5, 2.5 or 5 µM final concentration) and N-KhtT (2.5 or 10 µM final concentration) were added to everted vesicles prepared at pH 8.0 and the mixture incubated for 2 min before diluting it in assay buffer pH 7.5 or 8.5. Recombinant KhtT and KhtT$_{R110A}$ (both at 0.3, 0.6, 5 and 10 µM final concentration) were also added to everted vesicles prepared at pH 8.0 and the mixture incubated for 1 min before diluting it in assay buffer pH 7.5. All assays were performed at least in triplicate using a single batch of everted vesicles. c-di-AMP titrations were performed in at least quadruplicate, using 2 different batches of everted vesicles, except for the 3 lowest concentrations of c-di-AMP (12, 27 and 61 nM) used at pH 8.0, for which 3 measurements were performed using a single batch of vesicles. The rate of dequenching was determined by fitting the single-exponential equation $y = y_0 + A_1 e^{-(x-x_0)/\tau}$ (where A_1 is the amplitude and τ is the time constant) to experimental curves. Rate constants were determined from $1/\tau$. For the c-di-AMP titration experiments, rate constants were plotted as a function of c-di-AMP concentration and the Hill equation $y = Start + (End - Start) \times \frac{x^n}{K_{1/2}^n + x^n}$ (where *n* is the Hill coefficient) was fitted to these

data. For titrations at pH 7.5, we estimated the maximum rate from values of activity measured with KhtU-vesicles (0.007 s^{-1}) and fixed this value in the fitting of the Hill equation.

Analysis of the impact of c-di-AMP in KhtT:KhtU interaction

KhtU-vesicles (1.2 mg total protein) were incubated with 5 µM KhtT containing a C-terminal hexahistidine tag ($KhtT_{His}$) in WB assay buffer pH 7.0 (100 mM Bis-Tris propane pH 7.0, 140 mM KCl, 10 mM $MgCl_2$) for 1 h on ice. After centrifugation (1 h at 100,000 *g* and 4ºC), the pellet was gently resuspended in 300 µL of intermediate WB assay buffer pH 7.0 (20 mM Bis-Tris propane pH 7.0, 140 mM KCl, 10 mM $MgCl_2$). Resuspended vesicles (46 µL) were mixed with 50 µL of WB buffer with 3.6 mM nucleotide (c-di-AMP, c-di-GMP or no nucleotide) and with 800 µL of WB assay buffer pH 7.5 (100 mM Bis-Tris propane pH 7.5, 140 mM KCl, 10 mM $MgCl_2$) or pH 8.0 (100 mM Bis-Tris propane pH 8.0, 140 mM KCl, 10 mM $MgCl_2$). Mixtures were incubated on ice for 10 min and then centrifuged for 1 h at 100,000 *g* and 4ºC. After centrifugation, only 500 µL of the supernatant were collected and kept for analysis to avoid contamination with the pellet. Pellets were resuspended in 50 µL of their corresponding assay buffer. An identical experiment was performed with both empty and KhtU-vesicles in absence and in presence of c-di-AMP. Supernatant and pellet samples were analyzed by western blot, including everted membrane vesicles before and after $KhtT_{His}$ addition as negative and positive controls, respectively. Samples were separated in a 12% SDS-PAGE and electrophoretically transferred onto nitrocellulose membrane (Merck-Millipore) using a semi-wet electroblotting system (Bio-rad). Membrane was blocked in 5% (*w*/*v*) non-fat dry milk in 50 mM Tris-HCl pH 8.0, 150 mM NaCl, 0.2% (*v*/*v*) tween-20 (TBS-T) overnight at 4ºC, and subsequently incubated with anti-His antibody (1:2,500 in 5%-milk TBS-T) for 2 h at room temperature. After washing with TBS-T, membrane was incubated with HRP-conjugated secondary antibody (anti-mouse, 1:10,000 in 5%-milk TBS-T) for 1 h at room temperature. After a new washing with TBS-T, detection was done using ECL Prime Western Blotting System (GE Healthcare) and chemiluminescence detected with ChemiDoc XRS+ Imaging System (Bio-Rad).

Analysis of the contribution of N- and C-domains for KhtT:KhtU interaction

KhtU- or empty vesicles (200 µg total protein) were incubated with 2.5 µM $KhtT_{His}$, N_{His}-KhtT or C_{His}-KhtT in WB assay buffer 7.5 for 1h on ice. After centrifugation (1 h at 100,000 g and 4ºC), the pellet of vesicles was gently resuspended in 50 µL WB assay buffer and 900 µL of the same buffer was added before centrifugation as before. Pellets were resuspended in 50 µL of WB assay buffer pH 7.5 and were analyzed by western blot, including KhtU vesicles and their mixture with the proteins as negative and positive controls, respectively. Samples were separated in a 17% SDS-PAGE, electrophoretically transferred onto a PVDF membrane (Merck-Millipore) and proteins were detected as described above.

***B. subtilis* culture conditions**

For K^+ homeostasis experiments, *B. subtilis* strains 168 and Δ*khtU* (strain 168 in which *khtU* gene was replaced with a kanamycin cassette) were obtained from Bacillus Genetic Stock Center. These strains as well as Δ*khtU* transformed with empty pBS0E [Δ*khtU* (pBS0E)], pBS0E-*khtU* [Δ*khtU* (pBS0E-*khtU*)] or pBS0E-*khtTU* [Δ*khtU* (pBS0E-*khtTU*)] were grown in Spizizen Minimal Medium (SMM), containing 2 g L^{-1} $(NH_4)_2SO_4$, 1 g L^{-1} sodium citrate, 0.2 g L^{-1} $MgSO_4 \cdot 7H_2O$, 0.5% glucose, 50 mg L^{-1} tryptophan, 50 mg L^{-1} phenylalanine, 125 mg L^{-1} $MgCl_2 \cdot 6H_2O$, 7.3 mg L^{-1} $CaCl_2 \cdot 2H_2O$, 13.5 mg L^{-1} $FeCl_2 \cdot 6H_2O$, 1 mg L^{-1} $MnCl_2 \cdot 4H_2O$, 1.7 mg L^{-1} $ZnCl_2$, 0.43 mg L^{-1} $CuCl_2 \cdot 2H_2O$, 0.3 mg L^{-1} $CoCl_2$ and 0.6 mg L^{-1} $NaMoO_4 \cdot 2H_2O$). Ionic strength and osmolarity of the media were kept constant by varying the phosphate components (K_2HPO_4, KH_2PO_4, Na_2HPO_4 and NaH_2PO_4) so that 150 mM of monovalent cations (mixture of Na^+ and K^+) were present in all the solutions and pH was ~7.0. Pre-cultures (5ml) were grown in SMM with 2 or 100 mM K^+, 1 µg mL^{-1} erythromycin, 25 µg mL^{-1} lincomycin (for strains transformed with pBS0E-based vectors) and 7.5 µg mL^{-1} kanamycin (for

Δ*khtU* strains) at 37ºC and with 180 rpm agitation for 9 h. Three mL of SMM media, supplemented with antibiotics and 30 µg mL^{-1} bacitracin (for all strains) to induce protein expression, were inoculated so that initial OD_{600nm} of ~0.1. Growth continued at 37ºC, 200 rpm agitation for 10 h in media.

For experiments at different pH, *B. subtilis* strains Δ*khtU* (pBS0E), Δ*khtU* (pBS0E-*khtU*), Δ*khtU* (pBS0E-*khtTU*) and Δ*khtU* (pBS0E-$khtT_{R110A}U$) were grown in YPD medium (10 g L^{-1} yeast extract, 20 g L^{-1} peptone and 20 g L^{-1} dextrose) buffered with 100 mM of Bis-tris propane pH 7.0 or pH 9.0 with and without 100 mM KCl. Five milliliters cultures, containing 7.5 µg mL^{-1} kanamycin, 1 µg mL^{-1} erythromycin, 25 µg mL^{-1} lincomycin and 30 µg mL^{-1} bacitracin, were inoculated directly from a LB-K^+ (10 g L^{-1} tryptone, 5 g L^{-1} yeast extract and 5 g L^{-1} KCl) plate to an initial OD_{600nm} of ~0.2 and incubated at 37ºC with 180 rpm agitation for 8 h (at pH 7.0) or 12 h (at pH 9.0).

Determination of the expression levels of KhtT and $KhtT_{R110A}$ in *B. subtilis*

Relative expression levels of KhtT and $KhtT_{R110A}$ in Δ*khtU* (pBS0E-*khtTU*) and Δ*khtU* (pBS0E-$khtT_{R110A}U$) strains were estimated by peptide mass spectrometry analysis of cells extracts from Δ*khtU* (pBS0E), Δ*khtU* (pBS0E-*khtTU*) and Δ*khtU* (pBS0E-$khtT_{R110A}U$) strains grown in YPD medium adjusted to pH 7.0, since the *ΔkhtU* (pBS0E-$khtT_{R110A}U$) strain does not grow at pH 9.0.

Cells were inoculated directly from LB-K^+ plates into YPD medium supplemented with antibiotics (see section above) so that initial OD_{600nm} of ~0.1. Cultures were incubated at 37ºC with 130 rpm agitation until OD_{600nm} of ~0.25 at which point KCl was added to the growth media to a final concentration of 100 mM. At OD_{600nm} of 0.6-0.8, protein expression was induced by addition of bacitracin at 30 µg ml^{-1} and growth continued for 2 h. Cells were pelleted and kept at -20°C, until resuspension in 1 mL of 50 mM Tris pH 7.5, 100 mM NaCl, 1 mM magnesium acetate, 10 µg ml^{-1} lysozyme, 10 µg ml^{-1} DNase-I, protease inhibitors (EDTA-free mini-tablets from Pierce) and incubation on ice for 40 min. Samples were heated to 25°C for 5 min before adding 250 µL of 10% (*w*/*v*) SDS and vortexing. From each sample, 100 µL of cell extract were mixed with 50 µL 2x SDS-PAGE sample buffer with β-mercaptoethanol, vortexed, heated at 100°C and vortexed again before loading in a 17% SDS-PAGE. Purified recombinant KhtT and $KhtT_{R110A}$ proteins were also loaded as markers of migration. Proteins were visualized after coomassie staining and the molecular weight region equivalent to that of KhtT was sampled for peptide mass spectrometry analysis.

Gel samples were washed twice with 50% acetonitrile (ACN) in 50 mM triethylammonium bicarbonate (TEAB) with shaking for 5 minutes and further treated with ACN twice. Proteins were reduced with 25 mM DTT at 56ºC for 20 min and alkylated with 55 mM iodoacetamide (IAA) in the dark at room temperature for 20 min, followed by the same wash procedure. Proteins were then digested with trypsin (240 ng) in 50 mM TEAB, 0.01% surfactant at 50ºC for 60 min. Peptide gel extraction was performed with 2.5% trifluoroacetic acid (TFA) followed by 50% ACN, 0.1% TFA. Samples were dried out at the SpeedVac (Thermo Scientific), resuspended in 10 µL 0.1% TFA and cleaned by a C18 reverse phase chromatography following the manufacturer's instructions (ZipTip, Merck). Protein identification and quantification was performed by nano liquid chromatography mass spectrometry (nanoLC-MS/MS) as previously described (18) within a 90 minutes of chromatographic separation run. The LC separation was achieved by mixing solutions A (0.1% formic acid (FA)) and B (80% ACN, 0.1% FA) with the following gradient: 2.5 to 10% B (2 min), 10 to 35% B (50 min), 35 to 99% B (8 min), and a step of 99% B (10 min). Subsequently, the column was equilibrated with 2.5% B for 17 min. The specific MS parameters were: MS maximum injection time, 100 ms; dd settings: minimum AGC target 7×10^3, intensity threshold 6.4×10^4, and dynamic exclusion 20 s. Data acquisition was controlled by *Tune* 2.11 software (Thermo Scientific). The UniProt database 2020_06 (www.uniprot.org/) for *B. subtilis* strain 168 (Proteome ID UP000001570; 4,260 entries) together with the KhtT and $KhtT_{R110A}$ amino acid sequences were considered for protein identification. Protein quantification was performed by Label Free Quantification – LFQ, with precursor quantification based on intensity and normalization based on total peptide amount.

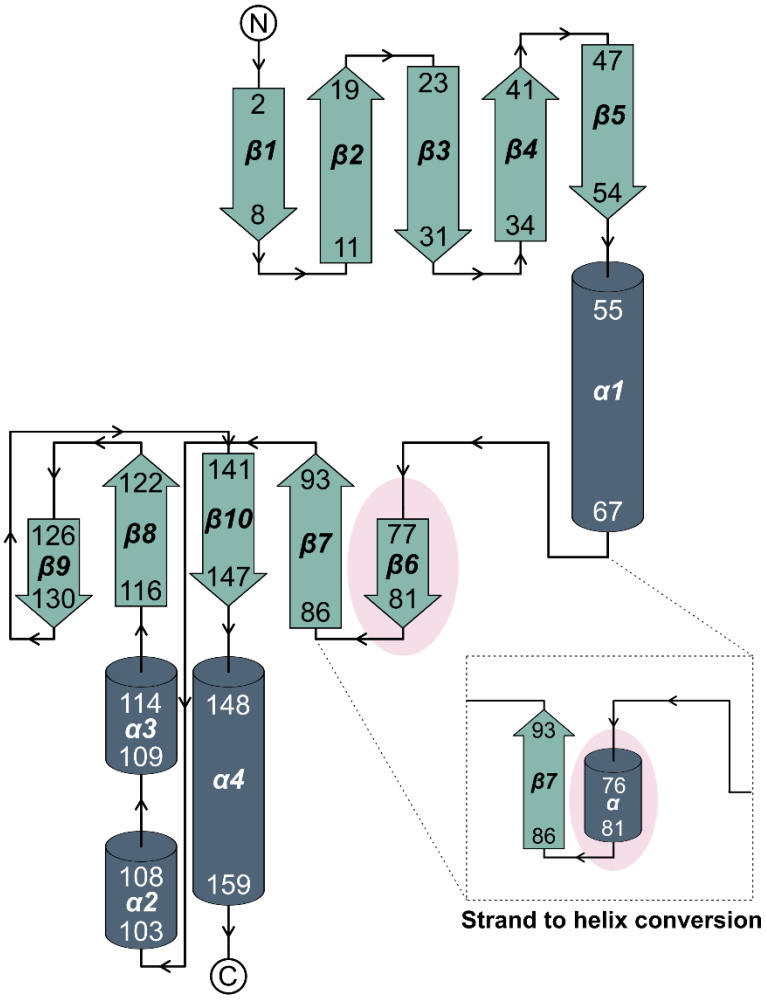

Fig. S1. Topology diagram of KhtT. Helices (α1-4), strands (β1-10) and N and C termini are represented by blue cylinders, green arrows, and circles, respectively. Secondary structure difference observed between high- and low-resolution structures of full-length KhtT in complex with c-di-AMP is indicated by pink ellipses.

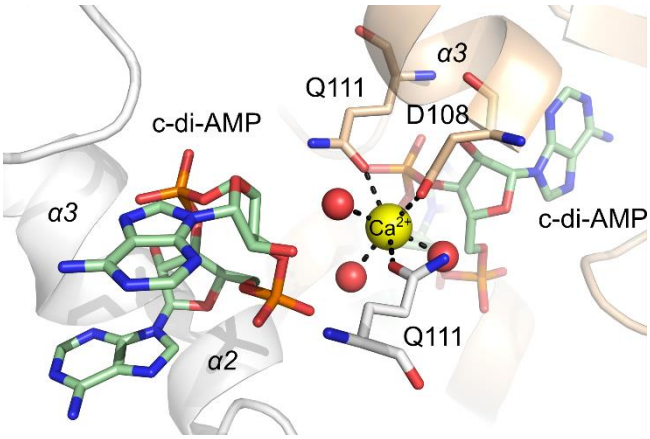

Fig. S2. Crystallographic contacts in the KhtT:c-di-AMP high-resolution structure. Close-up view of a crystallographic contact established near the c-di-AMP binding site. Crystallographically-related KhtT molecules are colored white or wheat. Respective c-di-AMP molecules are highlighted in pale green. Calcium ion at the interface is show as yellow sphere, coordinating water molecules are represented as red spheres and residues participating in Ca^{2+} coordination are represented by sticks.

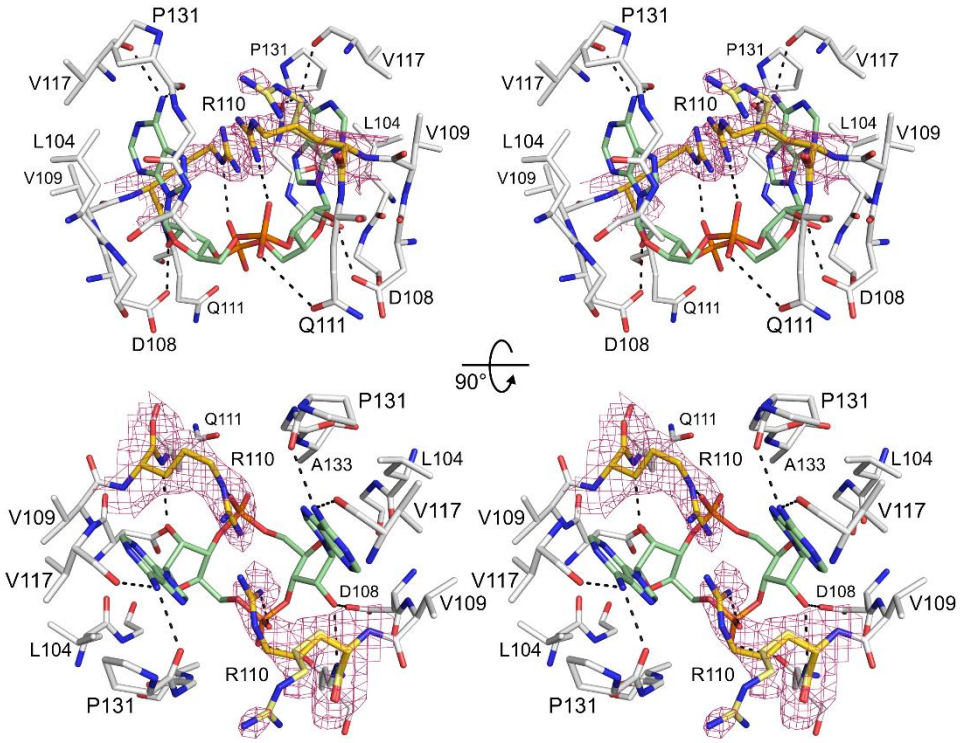

Fig. S3. Alternate c-di-AMP-binding mode. Stereo-view of the c-di-AMP binding site where Arg110 from molecules A and B (yellow sticks) participate in c-di-AMP binding. The alternative conformation of Arg110 with lower occupancy (39%) is shown in pale yellow. Electron density map around Arg110 residues (2mFo-DFc contoured at 1.0 σ) is shown as pink mesh. Hydrogen bonding is represented by dashed black lines. Upper and lower panels are rotated 90º around horizontal direction.

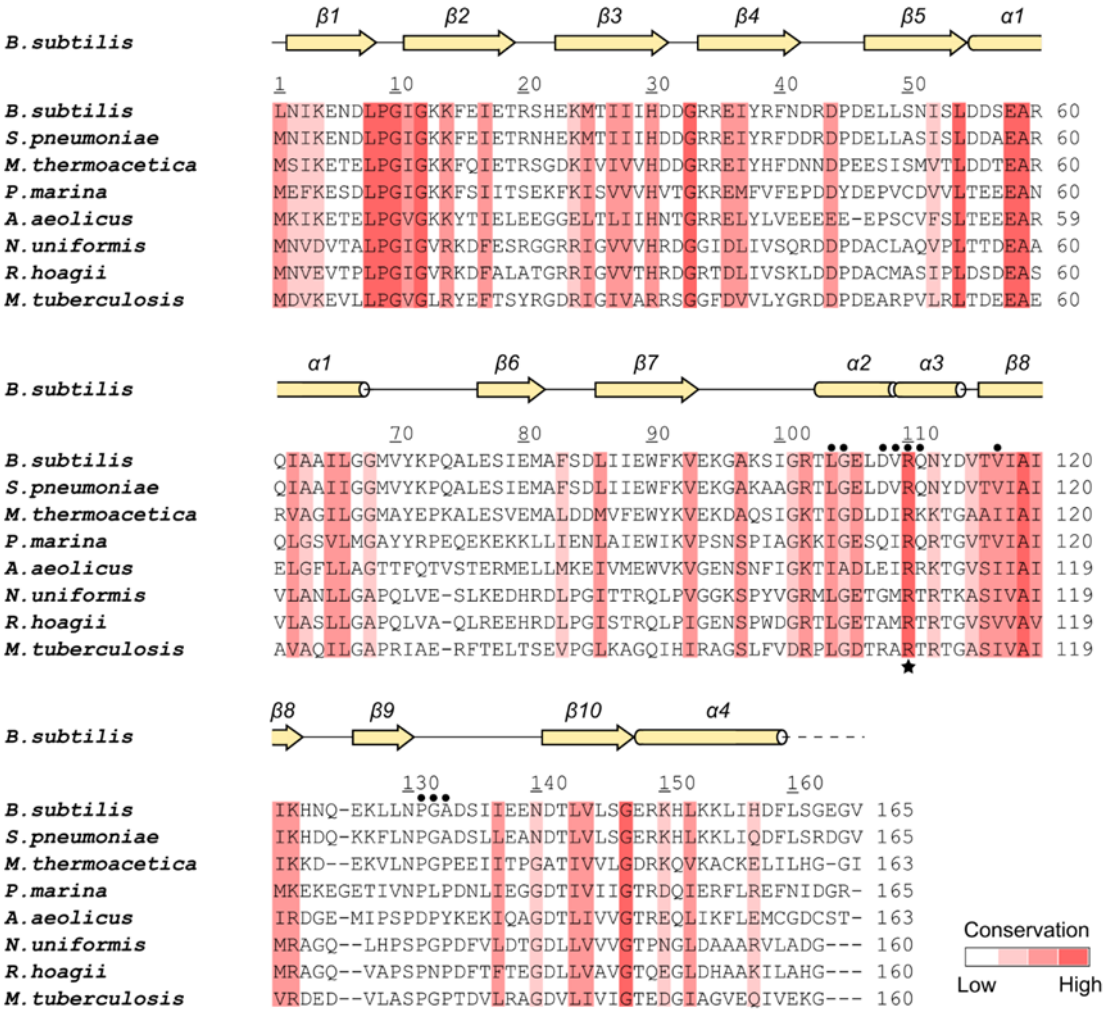

Fig. S4. Amino acid sequence alignment of KhtT homologs. Amino acid sequences of KhtT from *Bacillus subtilis* (NP_388867.1), *Streptococcus pneumoniae* (COD13704.1), *Moorella thermoacetica* (WP_025773296.1), *Persephonella marina* (WP_012676667.1), *Aquifex aeolicus* (WP_164930802.1), *Nocardia uniformis* (WP_067524522.1), *Rhodococcus hoagii* (WP_084968761.1) and *Mycobacterium tuberculosis* (WP_031746963.1) are aligned. Secondary structure elements of *B. subtilis* KhtT are indicated above the alignment. Residues involved in c-di-AMP binding are indicated by black dots, with the highly conserved Arg110 marked with a star.

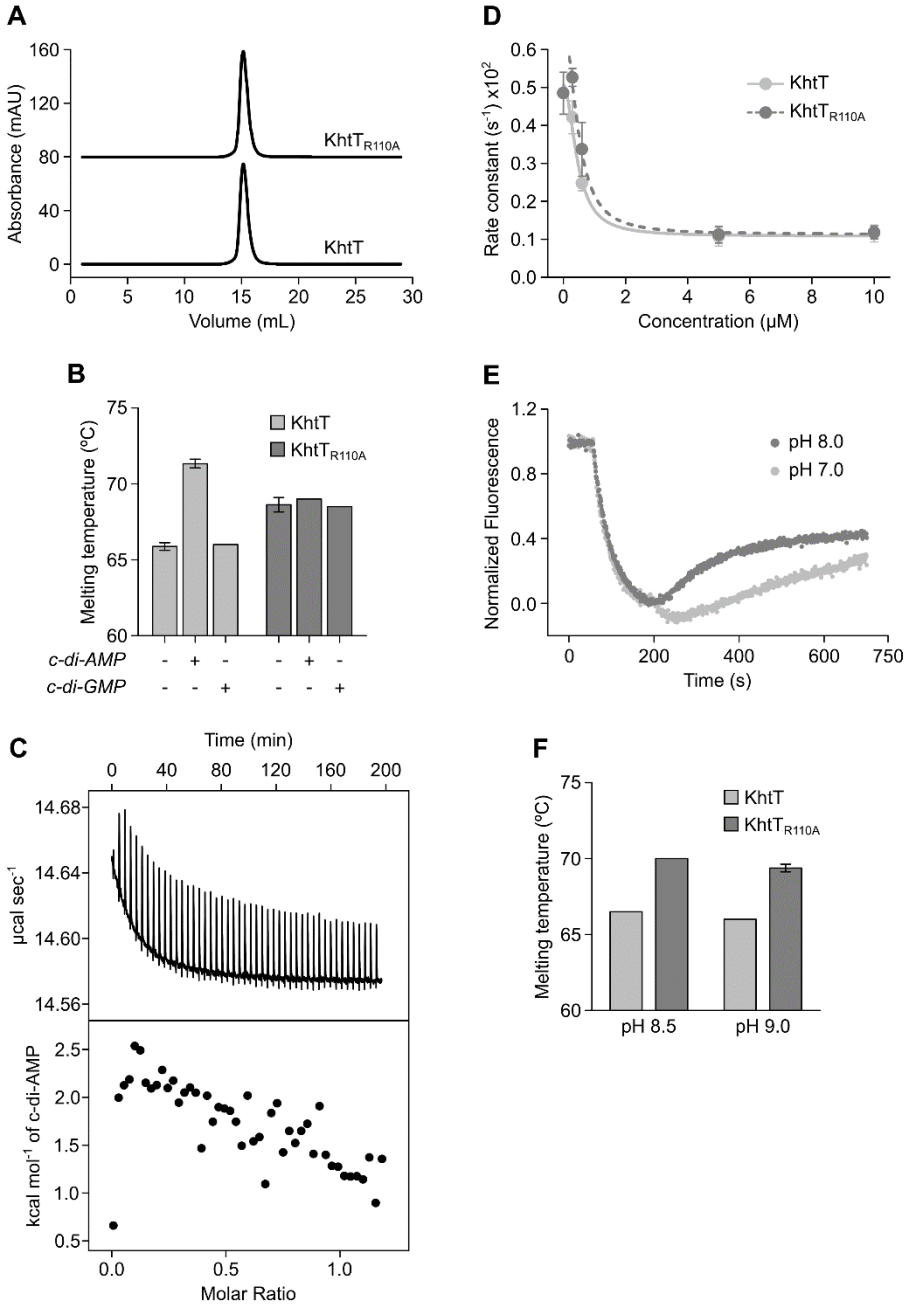

Fig. S5. Properties of KhtT$_{R110A}$ and KhtT$_{R110A}$U. (A) Size-exclusion chromatogram of purified KhtT and KhtT$_{R110A}$ showing identical elution profiles. (B) Plot of melting temperatures of KhtT and KhtT$_{R110A}$ in the absence and presence of c-di-AMP or c-di-GMP. While c-di-AMP increases the melting temperature (T_m) of KhtT by ~5ºC, indicating an interaction with the protein, this nucleotide produces no change in the KhtT$_{R110A}$ mutant. The KhtT$_{R110A}$ has higher thermal stability (T_m of 68.6 ± 0.5ºC) than KhtT (T_m of 65.9 ± 0.3ºC). Mean ± SD are shown. Error bars are not shown for measurements where all replicas have identical melting values. (C) Titration of c-di-AMP (133 μM) into KhtT$_{R110A}$ (17.5 μM) using ITC. Top panel shows the raw titration heat values plotted as a function of time and bottom panel shows normalized integration heat values plotted as a function of molar ratio. Experiment was performed at 25ºC. No binding of c-di-AMP to KhtT$_{R110A}$ was observed in the conditions tested. (D) Plot of rate constants measured from KhtU-vesicles titrated with increasing concentrations of KhtT (light gray) or KhtT$_{R110A}$ (dark gray). Data were fitted with Hill equation $= Start + (End - Start) \times \frac{x^n}{K_{1/2}^n + x^n}$, where *n* is the Hill coefficient and was kept fixed at

2 for both titrations. Estimation of constants of inhibition (or apparent dissociation) ($K_{1/2}$) for KhtT or $KhtT_{R110A}$ shows that both regulatory proteins interact and inhibit equally well KhtU. $K_{1/2}$ for KhtT is 0.46 ± 0.11 µM and for $KhtT_{R110A}$ 0.48 ± 0.58 µM. Mean ± SD are shown. (E) Representative fluorescence traces for $KhtT_{R110A}$U-vesicles prepared at pH 7.0 (light gray) or pH 8.0 (dark gray) and assayed under the same experimental conditions, at pH 7.5. Addition of 50 mM KCl caused a faster dequenching of fluorescence in the vesicles prepared at pH 8.0. (F) Plot of melting temperatures of KhtT and $KhtT_{R110A}$ at pH 8.5 and 9.0. The melting temperature of $KhtT_{R110A}$ is higher than KhtT by ~3ºC at both pHs. As the pH increases only a slightly decrease in the melting temperature of both proteins is observed. Mean ± SD are shown. Error bars are not shown for measurements where all replicas have identical melting values.

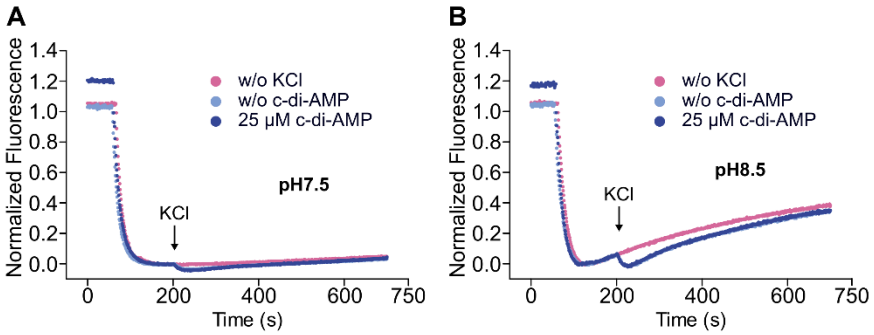

Fig. S6. c-di-AMP does not affect fluorescence in empty everted vesicles. Representative fluorescence traces for empty vesicles (prepared from cells transformed with empty pQE60) assayed at pH 7.5 (A) and 8.5 (B) in the absence (light blue) and in presence (dark blue) of 25 µM c-di-AMP. Nucleotide addition caused no change in the fluorescence dequenching profile. Addition of 50 mM of KCl induced a slightly quenching of the fluorescence both in presence and absence of c-di-AMP. Basal dequenching, in the absence of c-di-AMP and KCl, is shown in pink.

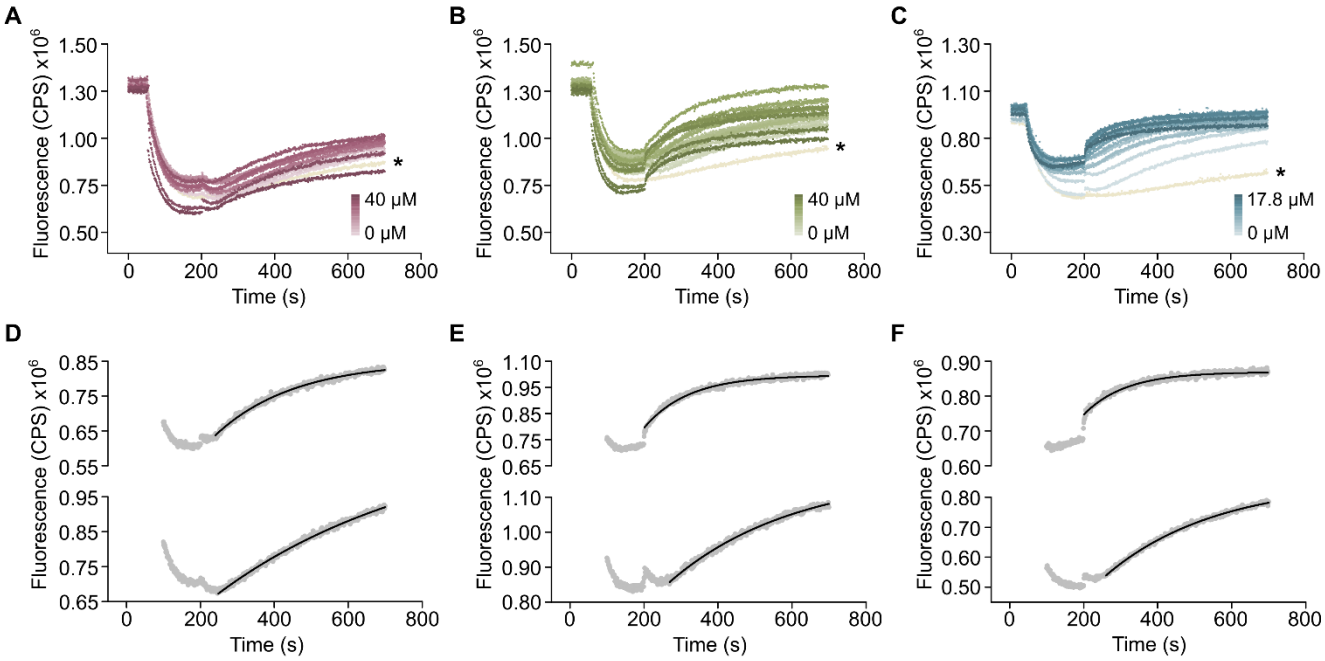

Fig. S7. Raw data from titration of c-di-AMP at various pHs. (A-C) Raw fluorescence data from representative titrations performed with KhtTU-vesicles in the presence of increasing concentrations of c-di-AMP (0 – 40 µM in A and B; and 0 – 17.8 µM in C) at pH 7.5 (A), 8.0 (B) and 8.5 (C). c-di-AMP concentration increases with the color intensity. The curve obtained with no addition of KCl is marked with an asterisk. (D-F) Representative experimental curves obtained at pH 7.5 (D), 8.0 (E) and 8.5 (F) for the lowest (0 µM, bottom data) and highest [40 µM (D and E) or 17.8 µM (F), top data] c-di-AMP concentrations are shown as gray dots. Single-exponential fits with equation $y = y_0 + A_1 e^{-(x-x_0)/\tau}$, where A_1 is the amplitude and τ is the time constant, are shown as black curves. Rate constants used in the main text were determined from $1/\tau$.

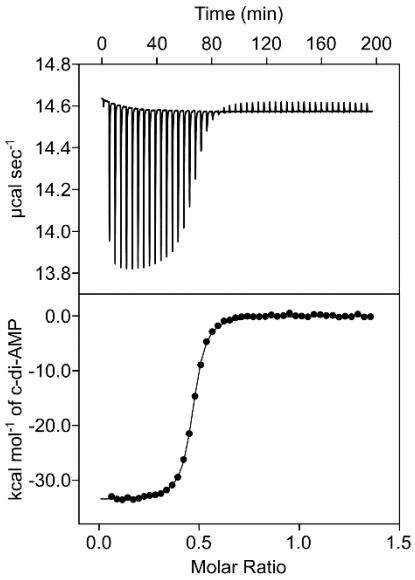

Fig. S8. Characterization of the interaction of c-di-AMP with KhtT at pH 7.5 using ITC. Titration of c-di-AMP (131 µM) into KhtT (15.8 µM) is shown. Top panel shows the raw titration heat values plotted as a function of time and bottom panel shows normalized integration heat values of injectant plotted as a function of molar ratio. Curve shown in bottom panel corresponds to a single-site binding model. Experiment was performed at 25ºC.

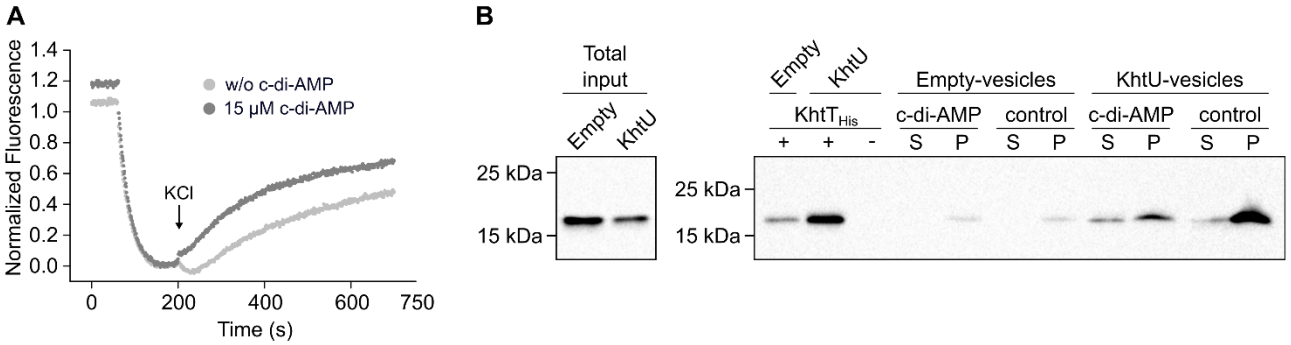

Fig. S9. KhtT$_{His}$U is activated by c-di-AMP. (A) Representative fluorescence traces for KhtT$_{His}$U-vesicles assayed at pH 8.5 in absence (light gray) and in presence (dark gray) of 15 µM c-di-AMP. Addition of 50 mM KCl caused a faster dequenching of fluorescence when c-di-AMP was present. (B) Western blot of the supernatant (S) and pellet (P) fractions from ultracentrifugation of empty or KhtU-vesicles after incubation with KhtT$_{His}$ at pH 7.5 with or without c-di-AMP. As shown before, c-di-AMP caused a reduction in the KhtT$_{His}$ associated with KhtU-vesicles. No changes were observed in the experiment with empty-vesicles. Importantly, the amount of KhtT$_{His}$ remaining in the KhtU-vesicles pellet fraction after incubation with c-di-AMP is higher than with empty-vesicles. KhtU-vesicles alone were loaded as negative control. Total input (mixture of empty- or KhtU-vesicles with KhtT$_{His}$) and the pellets of empty and KhtU-vesicles with KhtT$_{His}$ from first centrifugation (first two lanes in blot on the right) are shown as positive controls. Blot was probed with α anti-His.

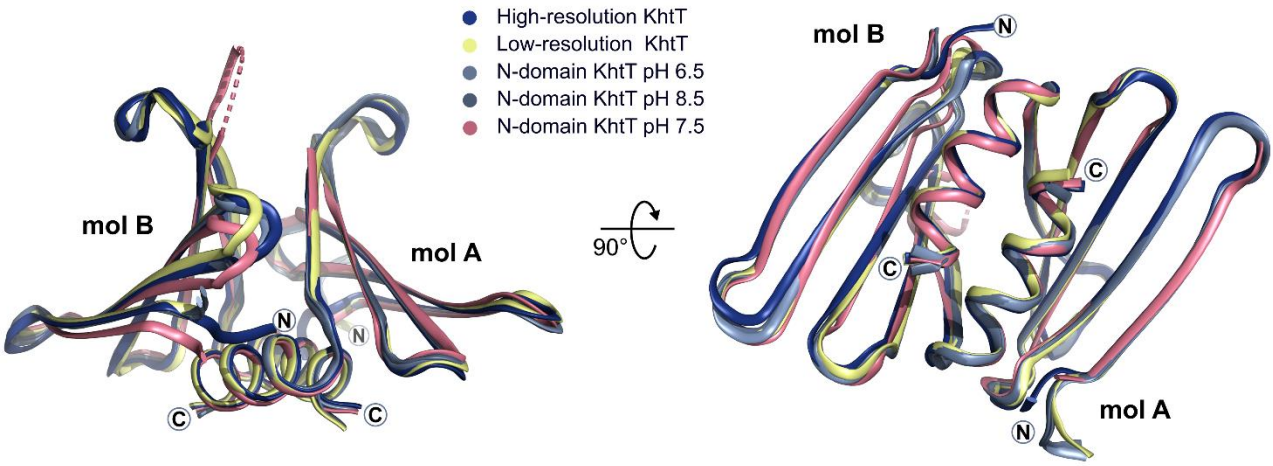

Fig. S10. Structures of the N-domain. Superposition of structures of the N-domain region of full-length KhtT structures (high and low-resolution) with those of N-domain alone (N-KhtT protein). While three structures (blue tones) are nicely superposed, small changes are observed for the low-resolution structure of the full-length KhtT (yellow) and N-KhtT pH 7.5 (pink). Molecules A and B in the dimer, as well as N and C termini are indicated. Left and right panels are rotated 90º around horizontal.

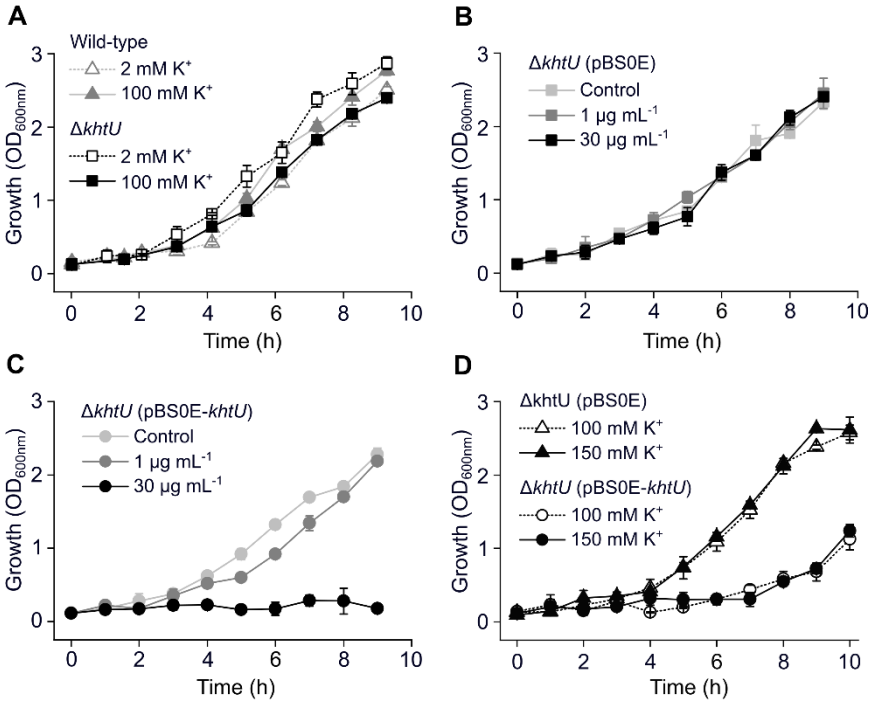

Fig. S11. Impact of *khtU* deletion, K^+ concentration and overexpression of KhtU in the growth of *B. subtilis*. (A) Optical density of strains 168 (wild-type) and Δ*khtU* growing in SMM with 2 or 100 mM K^+. No difference in growth phenotype was observed. (B-C) Optical density of strains Δ*khtU* (pBS0E) (B) and Δ*khtU* (pBS0E-*khtU*) (C) growing in SMM with 2 mM K^+ and without (control) or with 1 or 30 µg mL^{-1} bacitracin. Bacitracin had no impact in the growth of *B. subtilis* transformed with empty plasmid, Δ*khtU* (pBS0E), but increasing concentration of this antibiotic impaired the growth of the strain overexpressing KhtU, Δ*khtU* (pBS0E-*khtU*). (D) Optical density of strains Δ*khtU* (pBS0E) and Δ*khtU* (pBS0E-*khtU*) growing in SMM with 100 or 150 mM K^+. No difference in growth phenotype was observed. Mean ± SD of triplicate growths are shown.

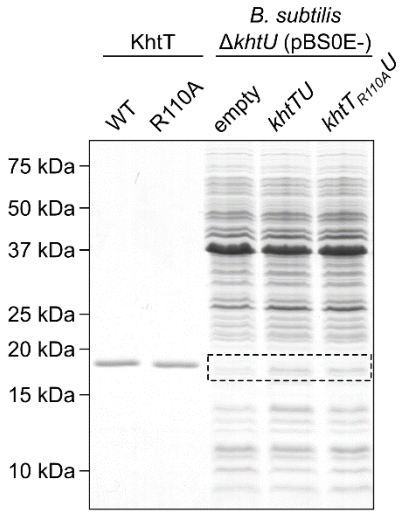

Fig. S12. SDS-PAGE of total protein extracts from *B. subtilis* strains. Total protein extracts from *B. subtilis* strains Δ*khtU* (pBS0E), Δ*khtU* (pBS0E-*khtTU*) and Δ*khtU* (pBS0E-*khtT*$_{R110A}$*U*) obtained after 2 h-induction of protein expression were separated in a 17% SDS-PAGE and visualized after coomassie staining. Purified recombinant KhtT and KhtT$_{R110A}$ (1 µg each) were used as markers of migration. The region sampled for mass spectrometry analysis is shown by a dashed rectangle.

Table S1. Data collection and refinement statistics.

Crystal	SeMet-KhtT:c-di-AMP complex	KhtT: c-di-AMP complex (High resolution)	KhtT: c-di-AMP complex (Low resolution)	N-domain KhtT pH 6.5	N-domain KhtT pH 8.5	N-domain KhtT pH 7.5
PDB code	-	7AGV	7AHM	7AGW	7AGY	7AHT
Data Collection						
Synchrotron radiation facility	SOLEIL	ALBA	ALBA	SOLEIL	SOLEIL	SOLEIL
Beamline	PROXIMA-1	XALOC	XALOC	PROXIMA-1	PROXIMA-1	PROXIMA-1
Wavelength (Å)	0.979180	0.979260	0.979260	0.978566	0.978566	0.978566
Reflections (measured/unique)	275,735/58,222	359,622/124,845	261,620/26,877	294,615/23,010	286,231/22,120	114,137/8,366
Space group	P 1 2_1 1	P 1 2_1 1	P 4_2 2 2	$P2_1$ 2_1 2_1	$P2_1$ 2_1 2_1	$P4_3$
a, *b*, *c* (Å)	72.8, 126.9, 81.7	72.9, 127.6, 81.9	190.7, 190.7, 84.6	34.7, 63.0, 65.3	35.2, 63.6, 64.6	48.5, 48.5, 66.7
α, *β*, *γ* (°)	90.0, 95.6, 90.0	90.0, 95.8, 90.0	90.0, 90.0, 90.0	90.0, 90.0, 90.0	90.0, 90.0, 90.0	90.0, 90.0, 90.0
Resolution (Å)	47.8 – 2.39	127.6 – 1.85	190.6 – 3.14	45.3 – 1.51	45.3 – 1.54	48.5 – 2.16
R_{merge}	0.073 (0.827)	0.033 (0.855)	0.175 (1.698)	0.044 (1.459)	0.051 (1.048)	0.048 (1.207)
$\langle I/\sigma(I) \rangle$	13.4 (1.6)	14.3 (1.3)	8.1 (1.1)	23.1 (1.7)	20.7 (1.6)	22.4 (2.4)
Half-set correlation $CC_{1/2}$	0.998 (0.672)	0.998 (0.514)	0.990 (0.714)	0.999 (0.786)	0.999 (0.910)	1.000 (0.943)
Completeness (%)	99.5 (96.0)	98.5 (99.1)	96.5 (99.8)	99.5 (93.5)	99.8 (100.0)	99.8 (99.4)
Multiplicity	4.7 (4.7)	2.9 (2.9)	9.7 (10.1)	12.8 (11.8)	12.9 (13.3)	13.6 (14.1)
Anomalous completeness (%)	96.0 (92.1)	-	-	-	-	-
Anomalous multiplicity	2.3 (2.4)	-	-	-	-	-
Half-set anomalous correlation $CC_{1/2}$	0.630 (0.000)	-	-	-	-	-
Refinement						
R_{work}/R_{free} (%)	26.8/33.0	20.4/24.2	23.7/27.2	22.2/24.5	22.5/23.4	24.5/27.9
Resolution	37.5 – 2.39	81.5 – 1.85	85.3 – 3.14	30.6 – 1.51	32.3 – 1.54	34.3 – 2.16
Total No. of atoms	9,565	11,278	5,226	1,253	1,240	980
No. of water molecules	38	480	0	75	75	0
R.m.s deviation						
Bond lengths (Å)	0.011	0.009	0.002	0.006	0.006	0.002
Bonds angles (°)	1.733	1.187	0.581	0.958	0.983	0.501
Ramachandran plot						
Favored (%)	80.0	96.7	93.6	100	99.3	97.4
Allowed (%)	10.9	3.2	6.4	0	0.7	2.6
Outliers (%)	9.1	0.1	0	0	0	0
Molecules in the asymmetric unit	8	8	4	2	2	2
Ligand	2BA	2BA	2BA	-	-	-

Values in parenthesis correspond to the outermost shell.

Table S2. Primers using in cloning and site-directed mutagenesis.

Primer name	Primer sequence 5'-3'
khtTU_pQE60_fw	TAGCTCCATGGGGAATATTAAAGAAAACGATCTGC
khtTU_pQE60_rv	TAGGTAGATCTTCATCCCTGTTTTTTTGCGGGCTG
khtT_pRSFDuet_fw	TAGCGGGATCCACTGGTGCCGCGCGGCAGCGGGTTGAATATTAAAG
khtT_pRSFDuet_rv	GTTAAGCGGCCGCTCACACGCCCTCTCC
khtU_pBS0E_fw	TCGCCTCTAGATCA*AGGAGG*AACTACTATGGACCATCTTGTATTTGAAG
khtU_pBS0E_rv	TCGCCCTGCAGTTATCCCTGTTTTTTTGCGGGCTGAAC
khtT_pBS0E_fw	TCGCCTCTAGATCA*AGGAGG*AACTACTTTGAATATTAAAGAAAACGATC
khtT_R110A_fw	CACTCGGTGAGCTTGATGTTGCCCAGAATTACGATGTCAC
khtT_R110A_rv	GTGACATCGTAATTCTGGGCAACATCAAGCTCACCGAGTG
khtT$_{His}$U_fw	CTGGAGAGGGCGTGGGATCCAGATCTCATCACCATCACCATCACTGAGCC CCGATGGAC
khtT$_{His}$U_rv	GTCCATCGGGGCTCAGTGATGGTGATGGTGATGAGATCTGGATCCCACGC CCTCTCCAG
N-KhtT-stop_fw	GCTATTCTCGGGGGCTAAGTCTATAAACC
N-KhtT-stop_rv	GGTTTATAGACTTAGCCCCCGAGAATAGC
N-KhtT_fw	TACTCCATGGGGAATATTAAAGAAAAC G
N-KhtT_rv	TGTTGCTCGAGGCCCCCGAGAATAGCTG
C-KhtT_fw	TACTCCATGGCTCTGGAGTCCATC
C-KhtT_rv	GTGGTGCTCGAGTCTGGATCCCACGCCCTCTCCAGAAAG

Bases underlined denote the enzymes restriction recognition sites used; bases in italics denote the ribosome binding site.

Table S3. Peptides of KhtT and KhtT$_{R110A}$ present in *B. subtilis* Δ*khtU* (pBS0E-*khtTU*) or Δ*khtU* (pBS0E-*khtT$_{R110A}$U*) extracts and identified by mass spectrometry. KhtT and KhtT$_{R110A}$ were among the 10 top most abundant proteins identified in the gel samples of Δ*khtU* (pBS0E-*khtTU*) and Δ*khtU* (pBS0E-*khtT$_{R110A}$U*) extracts, respectively. In contrast, the native KhtT protein in Δ*khtU* (pBS0E-*empty*) strain was found at much lower levels. Four peptides were mapped to KhtT that are unique in the proteome of *B. subtilis* strain 168. Two of these are shared by wild type and mutant KhtT (double underlined). The other two are present only in the mutant (single underlined). A peptide containing Arg110 (bold) was exclusively found in the *B. subtilis* Δ*khtU* (pBS0E-*khtTU*) extract, while two peptides containing an Ala (bold) replacing Arg110 were only identified in the extract of *B. subtilis* Δ*khtU* (pBS0E-*khtT$_{R110A}$U*).

Position	Sequence	Number of PSMs	
		Δ*khtU* (pBS0E-*khtTU*)	**Δ*khtU* (pBS0E-*khtT$_{R110A}$U*)**
[1-13]	MNIKENDLPGIGK	21	35
[1-14]	MNIKENDLPGIGKK	14	13
[5-13]	ENDLPGIGK	3	3
[5-14]	ENDLPGIGKK	1	-
[5-20]	ENDLPGIGKKFEIETR	-	5
[14-20]	KFEIETR	9	11
[25-34]	MTIIIHDDGR	1	-
[25-35]	MTIIIHDDGRR	5	39
[25-39]	MTIIIHDDGRREIYR	-	2
[36-60]	EIYRFNDRDPDELLSNISLDDSEAR	6	25
[40-60]	FNDRDPDELLSNISLDDSEAR	16	27
[44-60]	DPDELLSNISLDDSEAR	1	1
[103-110]	TLGELDV**R**	10	-
[103-122]	TLGELDV**A**QNYDVTVIAIIK	-	14
[103-127]	TLGELDV**A**QNYDVTVIAIIKHNQEK	-	7
[111-122]	QNYDVTVIAIIK	7	-
[123-149]	HNQEKLLNPGADSIIEENDTLVLSGER	-	10
[123-150]	HNQEKLLNPGADSIIEENDTLVLSGERK	-	3
[128-149]	LLNPGADSIIEENDTLVLSGER	16	28
[128-150]	LLNPGADSIIEENDTLVLSGERK	12	37
[154-165]	KLIHDFLSGEGV	7	38
[155-165]	LIHDFLSGEGV	9	26
Total number of peptide spectrum matches (PSMs) /Total number of identified peptides		138/16	324/18

SI References

1. Popp PF, Dotzler M, Radeck J, Bartels J, & Mascher T The Bacillus BioBrick Box 2.0: expanding the genetic toolbox for the standardized work with Bacillus subtilis. *Sci Rep* **7**, 15058 (2017).
2. Kabsch W Xds. *Acta Crystallogr D Biol Crystallogr* **66**, 125-132 (2010).
3. Winn MD, *et al.* Overview of the CCP4 suite and current developments. *Acta Crystallogr D Biol Crystallogr* **67**, 235-242 (2011).
4. Sheldrick GM Experimental phasing with SHELXC/D/E: combining chain tracing with density modification. *Acta Crystallogr D Biol Crystallogr* **66**, 479-485 (2010).
5. Kim H, *et al.* Structural Studies of Potassium Transport Protein KtrA Regulator of Conductance of K+ (RCK) C Domain in Complex with Cyclic Diadenosine Monophosphate (c-di-AMP). *J Biol Chem* **290**, 16393-16402 (2015).
6. Kleywegt GJ & Jones TA Software for handling macromolecular envelopes. *Acta Crystallogr D Biol Crystallogr* **55**, 941-944 (1999).
7. Emsley P, Lohkamp B, Scott WG, & Cowtan K Features and development of Coot. *Acta Crystallogr D Biol Crystallogr* **66**, 486-501 (2010).
8. Adams PD, *et al.* PHENIX: a comprehensive Python-based system for macromolecular structure solution. *Acta Crystallogr D Biol Crystallogr* **66**, 213-221 (2010).
9. McCoy AJ, *et al.* Phaser crystallographic software. *J Appl Crystallogr* **40**, 658-674 (2007).
10. Berman HM, *et al.* The Protein Data Bank. *Nucleic Acids Res* **28**, 235-242 (2000).
11. Krissinel E & Henrick K Secondary-structure matching (SSM), a new tool for fast protein structure alignment in three dimensions. *Acta Crystallogr D Biol Crystallogr* **60**, 2256-2268 (2004).
12. Hutchinson EG & Thornton JM PROMOTIF--a program to identify and analyze structural motifs in proteins. *Protein Sci* **5**, 212-220 (1996).
13. Krissinel E & Henrick K Inference of macromolecular assemblies from crystalline state. *J Mol Biol* **372**, 774-797 (2007).
14. Ashkenazy H, *et al.* ConSurf 2016: an improved methodology to estimate and visualize evolutionary conservation in macromolecules. *Nucleic Acids Res* **44**, W344-350 (2016).
15. McWilliam H, *et al.* Analysis Tool Web Services from the EMBL-EBI. *Nucleic Acids Res* **41**, W597-600 (2013).
16. Sievers F, *et al.* Fast, scalable generation of high-quality protein multiple sequence alignments using Clustal Omega. *Mol Syst Biol* **7**, 539 (2011).
17. Rosen BP & Tsuchiya T Preparation of everted membrane vesicles from Escherichia coli for the measurement of calcium transport. *Methods Enzymol* **56**, 233-241 (1979).
18. Osorio H, *et al.* Proteomics Analysis of Gastric Cancer Patients with Diabetes Mellitus. *J Clin Med* **10**, 407 (2021).